

Received August 12, 2016, accepted August 25, 2016, date of publication August 29, 2016, date of current version October 6, 2016.

Digital Object Identifier 10.1109/ACCESS.2016.2604078

Feasibility of Ambient RF Energy Harvesting for Self-Sustainable M2M Communications Using Transparent and Flexible Graphene Antennas

MICHAEL A. ANDERSSON¹, (Student Member, IEEE), AYÇA ÖZÇELIKKALE², (Member, IEEE), MARTIN JOHANSSON³, (Senior Member, IEEE), ULRICA ENGSTRÖM³, ANDREI VOROBIEV¹, AND JAN STAKE¹, (Senior Member, IEEE)

¹Terahertz and Millimetre Wave Laboratory, Department of Microtechnology and Nanoscience, Chalmers University of Technology, 412 96 Gothenburg, Sweden

²Department of Signals and Systems, Chalmers University of Technology, 412 96 Gothenburg, Sweden

³Ericsson Research, Ericsson AB, 417 56 Gothenburg, Sweden

Corresponding author: M. A. Andersson (andmic@chalmers.se)

This work was supported by VINNOVA through the SIO Grafen Program under Grant 2015-01439. The work of A. Özçelikkale was supported by the EU Marie Skłodowska-Curie Fellowship.

ABSTRACT Lifetime is a critical parameter in ubiquitous, battery-operated sensors for machine-to-machine (M2M) communication systems, an emerging part of the future Internet of Things. In this paper, the performance of radio frequency (RF) to DC energy converters using transparent and flexible rectennas based on graphene in an ambient RF energy-harvesting scenario is evaluated. Full-wave electromagnetic (EM) simulations of a dipole antenna assuming the reported state-of-the-art sheet resistance for few-layer, transparent graphene yields an estimated ohmic efficiency of 5%. In the power budget calculation, the low efficiency of transparent graphene antennas is an issue because of the relatively low amount of available ambient RF energy in the frequency bands of interest, which together sets an upper limit on the harvested energy available for the RF-powered device. Using a commercial diode rectifier and an off-the-shelf wireless system for sensor communication, the graphene-based solution provides only a limited battery lifetime extension. However, for ultra-low-power technologies currently at the research stage, more advantageous ambient energy levels, or other use cases with infrequent data transmission, graphene-based solutions may be more feasible.

INDEX TERMS Energy harvesting, flexible electronics, graphene, machine-to-machine communications, rectennas.

I. INTRODUCTION

In the future, it is envisaged that all devices that benefit from an Internet connection will be interconnected. In such a networked society, every citizen and company will be empowered to reach their full potential. Internet of Things (IoT) technology is a key enabler of this vision by delivering, for example, machine-to-machine (M2M) communication on a massive scale [1]. Information exchange between machines is already an important component in automated production, but in the future, areas such as smart energy distribution [2], health care [3] and smart cities [4] will also rely on Internet access. The market is now expanding toward both massive IoT deployment and more advanced solutions that may be categorized as critical IoT, as shown in Fig. 1. In massive IoT applications, such as sensors that report wirelessly to the cloud on a regular basis, the price of the communication

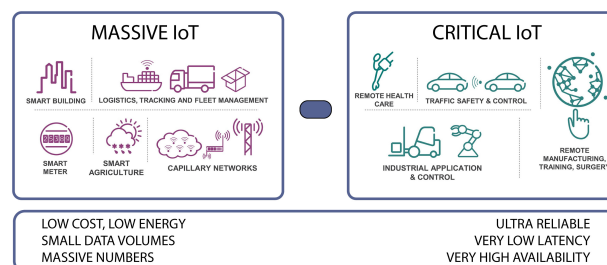


FIGURE 1. Application examples and requirements, massive vs. critical IoT [1].

link must be sufficiently low for the business case to make sense. In particular, the cost of the power supply is a great challenge in many wireless M2M applications, and there is an increasing demand for systems that are self-sustainable

or that offer extended battery lifetimes through the harvesting of energy [5]. Radio frequency (RF) signals represent an increasingly available and omnipresent energy source in urban environments [6]. Notably, the antenna and circuitry for recycling this ambient RF power can be made an integrated part of the M2M communication electronics.

However, there is a need for low-cost and eco-friendly antenna materials that are flexible and/or optically transparent to fully embody the ubiquitous potential of IoT [7], [8]. Flexible wireless sensors could be integrated as wearables in clothing or directly on the human body to monitor, for instance, the temperature, blood pressure and heart rate of patients on a continuous basis [3]. Arrays of RF energy harvesters that utilize transparent antennas, complemented with solar cells and applied on window glass, allow for energy-efficient day-and-night control of lighting and heating in buildings [4].

Graphene has a clear cost benefit due to the accessibility of carbon and is an eco-friendly alternative, particularly when applied on substrates such as paper [9] and textiles [10]. The potential use of recyclable substrates is important given the vast number of M2M nodes. Moreover, few-layer graphene is both flexible and offers a high degree of transparency given its conductivity [11], [12]. Together, these properties make graphene well suited given the requirements on the diversity and cost of an RF energy-harvesting antenna for M2M systems. Conversely, the demands are currently inaccessible using transparent antennas from indium tin oxide (ITO) [13], AgHT [14] or metal grids [15], which are brittle and expensive. Furthermore, graphene is a competitive option for passive and active electronics on flexible surfaces where oxide semiconductors, compound semiconductors and silicon all exhibit poor performance [16]. Rather, the main competitors for flexible and opaque antennas are additively printed metal-particle [17] and carbon-based inks [18]. Nevertheless, an all-carbon system could benefit from the integration of the antenna with graphene transistor rectifiers and the inherent suitability of graphene for sensing [19] and energy storage [20]. In addition, the field-effect allows tuning of the sheet resistance if a back-gate is available [11]. Consequently, a carbon-based system is a potentially low-cost and sustainable technology for diversified M2M systems.

In this practical article, we evaluate the feasibility of ambient RF energy harvesting in the common cellular communication frequency bands using a graphene antenna to improve the battery lifetime of sensors in massive IoT applications. In our envisioned scenario, invisible (to the human eye) graphene antennas can be applied on both flexible and rigid surfaces, e.g., paper [9], textiles [10] and plastics [21], for wearables and window glass. We estimate the energy harvested from ambient RF sources given a simulated state-of-the-art graphene antenna, which is truly transparent in contrast to reported simulations using copper ground planes [22], [23]. This is then converted to battery lifetime extensions, given the power consumption for different wireless transmission schemes, but excluding the details of the communication

channel [24]. In addition, the power management unit (PMU) and the energy storage [25] in the harvester circuit are also not addressed.

II. METHODS

This section describes the assumptions used in the power budget calculations. State-of-the-art reported available ambient RF power and graphene conductivity versus transparency are reviewed. Furthermore, the antenna simulations are detailed. Finally, the rectifier and transceiver parameters are discussed.

TABLE 1. Average and maximum ambient RF energy from base stations and WiFi Hotspots (London underground stations, 2012) [26].

Band	Frequency (MHz)	Average S_{BA} (nW/cm ²)	Maximum S_{BA} (nW/cm ²)
GSM900	925-960	36	1930
GSM1800	1805-1880	84	6390
3G	2110-2170	12	240
WiFi	2400-2500	0.18	6

A. AMBIENT RF ENERGY SOURCES

The cellular communication frequency bands provide a potentially omnipresent supply of ambient energy in urban scenarios. Here, the bands for GSM, 3G, LTE, and WiFi with frequencies between 900 MHz and 2.6 GHz are considered because these bands have the greatest amount of ambient energy. Table 1 summarizes the measured overall average and maximum intensity per band, S_{BA} , from base stations and WiFi hotspots at all underground stations in both suburban and urban areas in London, measured in the year 2012 using an omnidirectional antenna [26]. For the first three communication standards, only the down-link transmission bands are taken into account because these bands offer a relatively steady supply of energy over time. Note the close to one order of magnitude difference in the average and maximum values acquired. Although this implies that better energy-harvesting conditions could be obtained using dedicated RF sources [27], the latter are not considered in this paper. To be sure to cover the GSM1800 band with the highest energy level, a center frequency of 2 GHz is selected for the antenna design.

For comparison, a similar amount of power available from incoherent blackbody radiation poses several difficulties from a system perspective. In addition to the availability of a >300 °C object [28], the radiation to be collected and rectified is predominately emitted at frequencies above one terahertz.

B. GRAPHENE CONDUCTIVITY VERSUS TRANSPARENCY

Assuming applications in which a transparency of $>80\%$ is required, the number of graphene layers that can be used in an antenna is limited to <10 [29]. Consequently, this sets

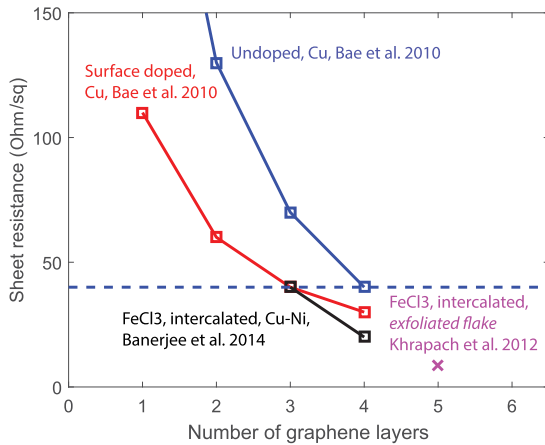


FIGURE 2. The DC sheet resistance versus number of layers for few-layer graphene grown by chemical vapor deposition on Cu and Cu-Ni with and without surface treatments to enhance conductivity [30]–[32].

a limit on the achievable sheet resistance (which is simply the inverse of the conductivity for a two-dimensional material). The state-of-the-art DC conductivities for large-area graphene grown by chemical vapor deposition (CVD) on a metal catalyst and transferred to insulating substrates are summarized in Fig. 2. Post-transfer surface treatment is applied to maximize the carrier concentration and minimize the sheet resistance. The CVD graphene is selected because it provides the best transparency for a certain sheet resistance, compared to ink-jet printed graphene for example [33], and it can be transferred to an arbitrary substrate. However, a slightly higher sheet resistance in the case of flexible plastics [30] and textile surfaces [10] have recently been reported. Because the CVD growth is self-limited to few layers, layer-by-layer transfer is required to reduce the sheet resistance. The accumulation of defects is responsible for the saturating improvement in the sheet resistance with the number of layers. The overall minimum value reported for transparent and flexible CVD-grown graphene in the literature is 20 Ω/sq for a 4-layer, FeCl_3 -intercalated graphene film [31]. In contrast to chemically surface-doped graphene, this intercalation has proven to be stable over long periods of time [32]. This is considerably better than the ultrathin (~ 5 nm) gold films that result in sheet resistance values $\sim 100 \Omega/\text{sq}$ combined with a lower transmittance than graphene of 75% [34] (cf. at the skin depth thickness of $2.5 \mu\text{m}$, gold has only $0.01 \Omega/\text{sq}$ at 2 GHz). However, micron-thick sputtered ITO films yield $< 5 \Omega/\text{sq}$ [13], and etched metal grids yield only $< 0.1 \Omega/\text{sq}$, both with 80% transmittance.

C. GRAPHENE DIPOLE ANTENNA SIMULATION

For simplicity, a linearly polarized planar on-wafer dipole antenna [35], [36] is used to investigate the influence of graphene conductivity on antenna performance. The antenna is simulated in Ansys HFSS as an ohmic sheet with a variable sheet resistance (i.e., not material specific to graphene) supported by a silicon wafer, as illustrated in Fig. 3. Theory [22]

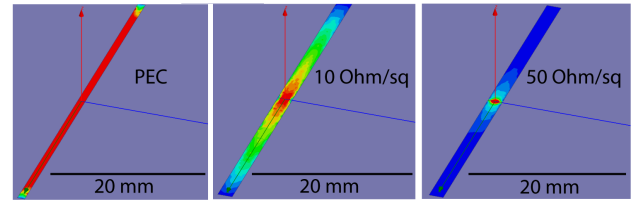


FIGURE 3. The surface currents on dipole antenna elements with the colored scale are the same in all three cases (from left to right) for a perfect electrical conductor (PEC), $R_{sh} = 10 \Omega/\text{sq}$ and $R_{sh} = 50 \Omega/\text{sq}$, respectively.

and experiment [37]–[39] both agree that at microwave frequencies the resistive part of the graphene impedance equals the DC value and that the imaginary part is negligible. The wafer is thin, and the antenna pattern (omnidirectional around the antenna axis) is very close to that of a free space dipole. Upon varying the sheet resistance, the radiation pattern does not change its shape, only the absolute levels. It is illustrative to inspect the surface currents in Fig. 3 for the antenna to observe how drastically the behavior changes, with only a moderate decrease in the conductivity. As a consequence of the large ohmic loss, a higher gain or a more broadband antenna (from a perfect electric conductor (PEC) perspective) is not considered as the improvement in system efficiency would be insignificant [35].

We assume that the antenna can be matched to a diode rectifier with an impedance in the low $k\Omega$ range for all considered sheet resistances given that $R_{ant} < 1 k\Omega$. The radiation efficiency (due solely to ohmic losses in the sheet) is used as a benchmark parameter, and it is found that a sheet resistance $< 40 \Omega/\text{sq}$ is required for an efficiency $> 1\%$. The full dependence is shown in Fig. 4. The state-of-the-art graphene provides 5% efficiency for the dipole antenna, which is comparable to the number in [22] for a graphene patch antenna. To further confirm the trend from the simulation, an experimental point (black cross) is inserted in Fig. 4 from a printed non-transparent graphite dipole antenna [18].

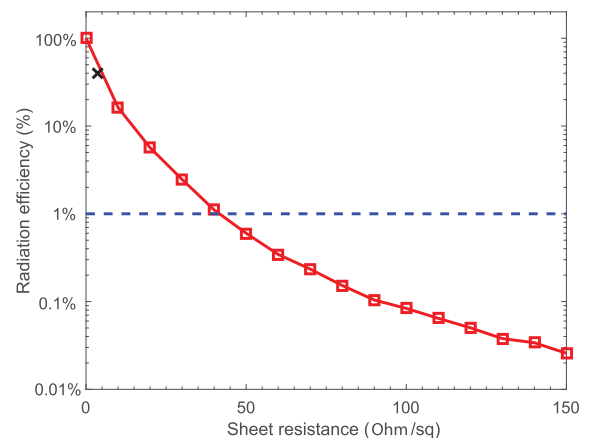


FIGURE 4. Antenna radiation efficiency at 2 GHz versus graphene sheet resistance. The black cross shows an experimental confirmation of the simulated trend from a non-transparent graphite dipole antenna of [18].

D. PERFORMANCE OF RF-TO-DC DIODE RECTIFIERS

The estimated RF power received at the antenna terminals is the product of the assumed input ambient RF energy and the simulated antenna gain or effective area as [35]

$$P_{rec} = A_{eff} \cdot S_{BA} = \frac{G \cdot \lambda^2}{4\pi} \cdot S_{BA}, \quad (1)$$

where λ is the wavelength and G is the antenna gain. Because the antenna orientation is arbitrary relative to the incoming radiation, the average gain over all pointing directions must be used. This essentially corresponds to an omnidirectional antenna with the same ohmic efficiency, which is required to match the antenna used in collecting the ambient intensity data [26]. To account for polarization in a fading urban environment, two perpendicularly polarized dipoles can be employed [40].

The resulting output DC power is given proportionally from the input received RF power by the rectifier efficiency, η_r , from $P_{DC} = \eta_r \cdot P_{rec}$. Considering the low graphene sheet resistance required and the wide metal-graphene contact periphery to the antenna, we regard the influence of the metal-graphene interface to be negligible. The rectifier efficiency is linearly dependent on the RF input power. Considering a single diode (or diode connected field effect transistor), it is [41]

$$\begin{aligned} \eta_r &= \mathcal{R}_I^2 \frac{P_{rec} \eta_m^2 R_j}{4 \left(1 + \omega^2 C_j^2 R_j R_s \right)} \simeq \mathcal{R}_I^2 \frac{P_{rec} \eta_m^2 R_j}{4} \\ &= \mathcal{R}_V^2 \frac{P_{rec} \eta_m^2}{4 R_j}. \end{aligned} \quad (2)$$

In the above expression, \mathcal{R}_I and \mathcal{R}_V are the (short circuit) current and (open circuit) voltage responsivity, respectively. Furthermore, η_m is the antenna to rectifier impedance matching coefficient, R_j is the junction or differential channel resistance (assumed to be equal to the load resistance R_L), $\omega = 2\pi f$ is the frequency, and R_s is the parasitic series resistance. This expression is valid under the condition that $R_s \ll R_j$. A comparison of the performance between a graphene transistor, which would allow for an all-graphene integrated system, and commercial Schottky diodes is presented in Fig. 5 based on (2). Schottky diodes are fundamentally limited to $\mathcal{R}_I = 19.4$ A/W (which is closely achieved in practice). The small nonlinearity of the current in a graphene FET (GFET), however, makes them practically limited to $\mathcal{R}_I \sim 1$ A/W [42], [43]. State-of-the-art for all solid-state detectors in Fig. 5 are the Sb backward diodes with $\mathcal{R}_I \simeq 23.5$ A/W [44], [45]. Deviations from (2) occur at higher input power levels where the small-signal approximation is not valid, as indicated by the solid line in Fig. 5.

In the following, we consider diode-based rectifiers because their efficiency is up to two orders of magnitude higher than that for current CVD GFETs. Actual reported diode rectifiers realized with RF energy harvesting in mind provide efficiencies of 40%, 20% and 5% at 100 μ W, 10 μ W and 1 μ W of received power at the matched antenna

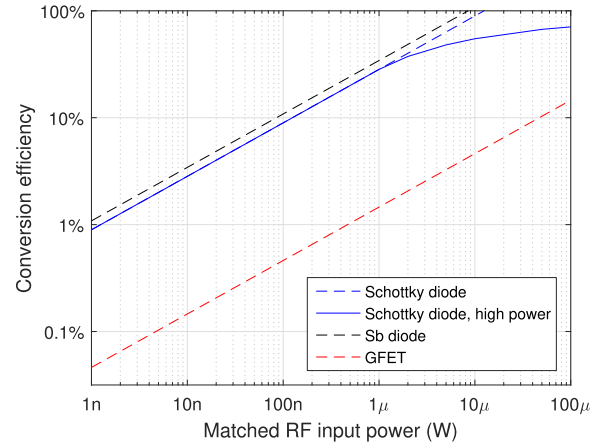


FIGURE 5. Rectifier efficiency, Schottky diodes are limited to $\mathcal{R}_I = 19.4$ A/W, Sb diodes to $\mathcal{R}_I = 23.5$ A/W and reported GFETs have $\mathcal{R}_I \sim 1$ A/W.

terminals [46], respectively, corresponding well with the high input power in Fig. 5.

E. POWER CONSUMPTION FOR THE TRANSCIVER AT THE SENSOR

The above subsections provided one end of the power-budget calculation. Now the other end is considered: the DC power consumption by the sensor operations for which the harvested power will be used. Due to the high energy cost of operating a transceiver circuit, we focus on the energy expenditure for communications. We consider the M2M communication scenarios and associated power consumption model in [47]: the transceiver is operated in discontinuous reception (DRX) mode, periodically listening for control signals. At regular intervals, the transceiver is turned on to communicate the sensor reading, but it is off for a vast majority of the time to save power. Short bursts of data are sent with reporting time intervals of hours or days. Each packet is assumed to be on the order of 1 kbyte or less in size, consistent with [47] and the nature of the M2M sensor communications considered here.

The implemented model is illustrated in Fig. 6. Descriptions of the power consumptions and durations for the different periods (or phases) of the DRX scenario are listed below.

- *Active*, receiving data from a data center (P_{act} , t_{act})
- *Nonactive*, transceiver turned OFF (sleeping mode) to conserve energy (P_{sleep} , t_{DRX})

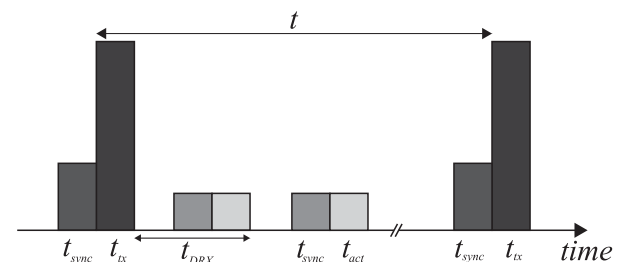


FIGURE 6. Model for the transceiver to be powered by RF energy harvester [47].

TABLE 2. Parameters used to calculate the DC power consumption for the off-the-shelf [47] and ultra-low-power [48] transceivers.

Transceiver	P_{tx} (mW)	P_{act} (mW)	P_{clock} (mW)	P_{base} (mW)	P_{sleep} (pW)	t_{act} (ms)	$t_{sync}(ms)$	t_{DRX} (ms)
Off-the-shelf [47]	300	100	10	0.01	0	10	10	t
Ultra-low-power [48]	0.19	0.06	0.006	-	40	10	10	t

- *Transmission*, sensor data reading sent (P_{tx} , t_{tx})
- *Sync*, establishing contact with data center before active or transmission periods (P_{clock} , t_{sync})

We make the most conservative assumption that the transceiver is turned ON to receive instructions at the same interval as the transmission is occurring, i.e., the reporting time $t = t_{DRX}$.

Hereafter, two cases are considered in the power-budget calculations. The first is an off-the-shelf transceiver example with estimated performance as of year 2020 [47]. The second is an ultra-low-power transceiver demonstrated at a research institution, with a power-optimized design in terms of both transmitter power and in particular a very low parasitic sleep power [48]. The powers and durations used for the two scenarios are compared in Table 2. Note that the reported sleep power in [48] includes the base power, which is considered as a separate item in [47]. In the limit of a long reporting interval, the effects of sleep and base powers in the consumption model converge. Thus, as a consequence of the high base power, the off-the-shelf device will still have a higher power consumption than the ultra-low-power design at rest.

III. RESULTS

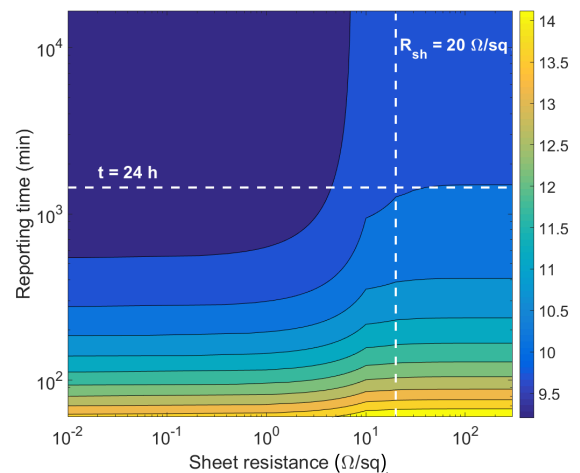
In this section, we present to what extent the RF energy harvester could prolong the battery lifetime of the sensor and whether it could make it completely self-sustainable. In addition to the power consumption, the outcome relies both directly and indirectly on the assumed available ambient intensity, S_{BA} (cf. the average and maximum values for each frequency band in Table 1). This is because the harvested power depends on the input as $P_{DC} = \eta_r \cdot A_{eff} \cdot S_{BA}$ and because a higher received RF power significantly increases the rectifier efficiency compared to low input power levels. In all the cases presented below, the summed received power across all the communication bands in Table 1 is used. The received power is calculated separately in each band taking into consideration the slightly non-constant antenna gain. The rectifier efficiency is assumed to be $\eta_r = 50\%$, which is to a certain extent optimistic for RF input powers from the antenna at the lower end of the scale. Nevertheless, integrated rectifier circuits [49] with, for instance, special PMUs [50] have been reported to achieve high efficiency also in the low- μ W power range. The three main situations investigated are listed below.

- Case #1 - Average S_{BA} and off-the-shelf transceiver (most conservative parameter set)

- Case #2 - Average S_{BA} and ultra-low-power transceiver (relaxed assumption with respect to energy consumption)
- Case #3 - Maximum S_{BA} and off-the-shelf transceiver (optimistic assumption with respect to energy availability)

A. CASE #1 - CONSERVATIVE PARAMETER SET

First, we consider both the average available power for harvesting [26] and the power consumption of an off-the-shelf transceiver, as shown in Table 2 [47]. In this case even a skin depth limited metal dipole antenna results in a minimal increase in the battery lifetime and still provides a high net power consumption even with very long reporting intervals, as shown in Fig. 7. Accordingly, neither the sheet resistance of state-of-the-art transparent but non-flexible ITO [13] and metal grids [15] nor state-of-the-art flexible but non-transparent printed silver nanoparticle thin-films [17] are good enough. If a transparent graphene antenna is employed, even with a state-of-the-art sheet resistance, the enhancement in battery lifetime is negligible, as shown in Fig. 8.

**FIGURE 7.** Net power consumption (μ W) for a predicted off-the-shelf transceiver as of year 2020 [47] and the average ambient RF intensity [26].

B. CASE #2 - RELAXED CONSUMPTION ASSUMPTION

Second, we consider the average available power for harvesting [26], but using a transceiver with an ultra-low power consumption, as shown in Table 2 [48]. Now, the best envisioned graphene antenna could also be used to fully power the system

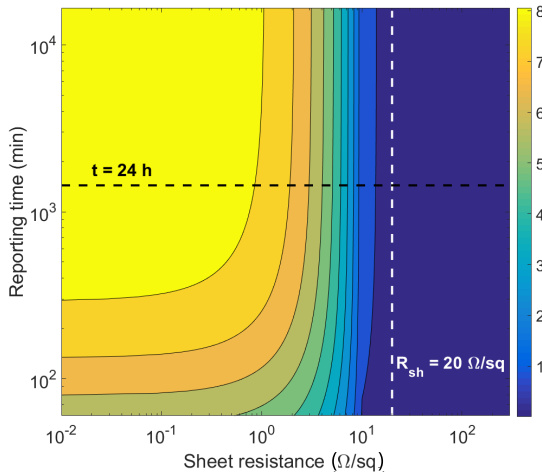


FIGURE 8. Relative battery lifetime increase as a percentage for an off-the-shelf transceiver as of year 2020 [47] and the average ambient RF intensity [26].

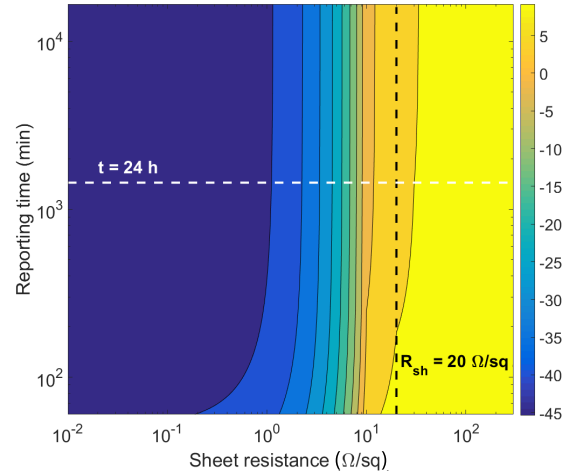


FIGURE 10. Net power consumption (μW) for a predicted off-the-shelf transceiver as of year 2020 [47] and the maximum ambient RF intensity [26].

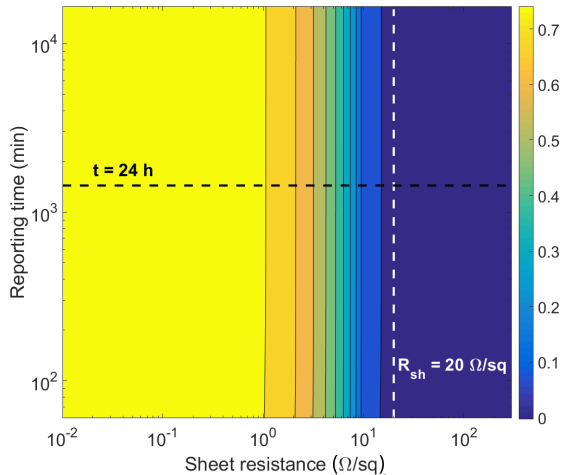


FIGURE 9. Net power production (μW) for an ultra-low-power transceiver [48] and the average ambient RF intensity [26].

even without a battery and having a reporting frequency of several times per day. This is shown in Fig. 9, which presents the net power production. For a self-sustainable system under these conditions, the requirement is that the graphene sheet resistance only needs to reach a value $<100 \Omega/\text{sq}$. This conductivity can be satisfied for transparent graphene even under bent operating conditions [30].

C. CASE #3 - RELAXED PRODUCTION ASSUMPTION

Third, we consider the deployment of the sensor at a location where the maximum ambient power for harvesting is available [26]. Now, both a transparent metal grid antenna [15] and a flexible printed silver dipole antenna [17] enable an off-the-shelf transceiver [47] to be self-sustainable with the year 2020 consumption and a reporting interval of several times per day. However, in a scenario in which only flexibility is required, printed carbon could instead be the material of

choice for the antenna [18]. Furthermore, a state-of-the-art transparent graphene antenna provides a decent 30% battery lifetime increase, as shown in Fig. 10. The consumption of the transceiver with the employed reporting scheme is $\sim 10 \mu\text{W}$ on average.

D. ESTIMATED BATTERY LIFETIMES FOR TRANSCIVER

Considering the three main cases above, it is also of interest to compare the absolute numbers for the battery lifetimes, particularly for the current off-the-shelf transceiver. This requires $\sim 10 \mu\text{W}$ DC power on average, with the reporting model used in case #1 and case #3. Let us consider the case in which the battery capacity is $6500 \text{ J} \approx 2 \text{ Wh}$ (equivalent to one AA battery), on the assumption that there is no battery self-discharge and that the best possible envisioned transparent graphene antenna is used. Then, with a $t = 24 \text{ h}$ reporting interval, the average power consumption provides a very long battery lifetime even without employing any RF energy harvesting. The actual numbers for all the different cases are presented in Table 3, also including case #2.

TABLE 3. Battery lifetime comparison with 2 Wh capacity for the three listed scenarios using a state-of-the-art graphene antenna.

Parameter set	No RF harvesting	#1	#2	#3
Battery lifetime (yrs.)	20	20	∞	26

IV. CONCLUSIONS

This study has examined the viability of using graphene rectennas in optically transparent RF-to-DC energy converters on rigid and flexible surfaces for ambient RF energy harvesting to power, entirely or partially, sensor nodes in wireless Massive M2M communication networks. Full-wave EM simulations using the state-of-the-art sheet resistance for transparent graphene provides a dipole antenna ohmic efficiency

of 5%. Based on the low graphene antenna efficiency, the harvested power in the power budget example was in the range of only 1 to 50 μ W from the conservative average value to the more optimistic maximum value on the reported ambient RF intensity in urban and suburban environments. In the calculations, a diode-based rectifier was assumed, as the graphene transistor rectifier efficiency is currently far inferior.

Altogether, the sensor reporting interval in a DRX scheme then needs to be on the order of one day to offer a significant improvement in battery lifetime. This is a relevant reporting time scale for various envisioned sensors in future massive M2M systems. Nevertheless, under conservative conditions for ambient RF energy levels and an off-the-shelf transceiver, the current graphene rectenna usefulness would be minimal. However, a graphene antenna could be a possible option under favorable conditions on available power or in a future scenario in which current ultra-low-power, proof-of-concept transceivers have been commercialized. Specifically, at long reporting intervals, the transceiver base power consumption is a key parameter for a self-sustainable sensor to be feasible with the currently best graphene dipole antenna. Provided that a simultaneous hundred-fold decrease in the transmission power is possible, the base power consumption needs to be reduced by at least three orders of magnitude from current off-the-shelf transceivers. However, obtaining an order of magnitude lower sheet resistance for transparent CVD graphene, i.e., an order of magnitude higher antenna efficiency, remains unreachable. To make graphene compete with state-of-the-art transparent metal grid antennas is thus extremely challenging. In applications that require flexibility but not transparency, however, ink-jet-printed carbon antennas constitute a favorable alternative.

REFERENCES

- [1] Ericsson AB. (2016). *Cellular networks for Massive IoT—Enabling Low Power Wide Area Applications*. [Online]. Available: http://www.ericsson.com/res/docs/whitepapers/wp_iot.pdf
- [2] J. Pan, R. Jain, S. Paul, T. Vu, A. Saifullah, and M. Sha, "An Internet of Things framework for smart energy in buildings: Designs, prototype, and experiments," *IEEE Internet Things J.*, vol. 2, no. 6, pp. 527–537, Dec. 2015.
- [3] S. M. R. Islam, D. Kwak, M. H. Kabir, M. Hossain, and K.-S. Kwak, "The Internet of Things for health care: A comprehensive survey," *IEEE Access*, vol. 3, pp. 678–708, 2015.
- [4] A. Zanella, N. Bui, A. Castellani, L. Vangelista, and M. Zorzi, "Internet of Things for smart cities," *IEEE Internet Things J.*, vol. 1, no. 1, pp. 22–32, Feb. 2014.
- [5] S. Kim *et al.*, "Ambient RF energy-harvesting technologies for self-sustainable standalone wireless sensor platforms," *Proc. IEEE*, vol. 102, no. 11, pp. 1649–1666, Nov. 2014.
- [6] C. R. Valenta and G. D. Durgin, "Harvesting wireless power: Survey of energy-harvester conversion efficiency in far-field, wireless power transfer systems," *IEEE Microw. Mag.*, vol. 15, no. 4, pp. 108–120, Jun. 2014.
- [7] L. Roselli *et al.*, "Smart surfaces: Large area electronics systems for Internet of Things enabled by energy harvesting," *Proc. IEEE*, vol. 102, no. 11, pp. 1723–1746, Nov. 2014.
- [8] A. Nathan *et al.*, "Flexible electronics: The next ubiquitous platform," *Proc. IEEE*, vol. 100, pp. 1486–1517, May 2012.
- [9] S. Kumar, S. Kaushik, R. Pratap, and S. Raghavan, "Graphene on paper: A simple, low-cost chemical sensing platform," *ACS Appl. Mater. Interfaces*, vol. 7, no. 4, pp. 2189–2194, Jan. 2015.
- [10] A. I. S. Neves *et al.*, "Transparent conductive graphene textile fibers," *Sci. Rep.*, vol. 5, pp. 9866–1–9866–7, May 2015.
- [11] K. S. Novoselov *et al.*, "Electric field effect in atomically thin carbon films," *Science*, vol. 306, no. 5696, pp. 666–669, 2004.
- [12] A. C. Ferrari *et al.*, "Science and technology roadmap for graphene, related two-dimensional crystals, and hybrid systems," *Nanoscale*, vol. 7, no. 11, pp. 4598–4810, Sep. 2015.
- [13] N. Outaleb, J. Pinel, M. Drissi, and O. Bonnaud, "Microwave planar antenna with RF-sputtered indium tin oxide films," *Microw. Opt. Technol. Lett.*, vol. 24, no. 1, pp. 3–7, 2000.
- [14] T. Peter, T. A. Rahman, S. W. Cheung, R. Nilavalan, H. F. Abutarboush, and A. Vilches, "A novel transparent UWB antenna for photovoltaic solar panel integration and RF energy harvesting," *IEEE Trans. Antennas Propag.*, vol. 62, no. 4, pp. 1844–1853, Apr. 2014.
- [15] J. Hautcoeur, F. Colombel, X. Castel, M. Himdi, and E. M. Cruz, "Optically transparent monopole antenna with high radiation efficiency manufactured with silver grid layer (AgGL)," *Electron. Lett.*, vol. 45, no. 20, pp. 1014–1016, Sep. 2009.
- [16] Y. Liang, X. Liang, Z. Zhang, W. Li, X. Huo, and L. Peng, "High mobility flexible graphene field-effect transistors and bipolar radio-frequency circuits," *Nanoscale*, vol. 7, no. 25, pp. 10954–10962, May 2015.
- [17] J. Bito, J. G. Hester, and M. M. Tentzeris, "Ambient RF energy harvesting from a two-way talk radio for flexible wearable wireless sensor devices utilizing inkjet printing technologies," *IEEE Trans. Microw. Theory Techn.*, vol. 63, no. 12, pp. 4533–4543, Dec. 2015.
- [18] X. Huang *et al.*, "Binder-free highly conductive graphene laminate for low cost printed radio frequency applications," *Appl. Phys. Lett.*, vol. 106, no. 20, pp. 203105–1–203105–4, 2015.
- [19] E. W. Hill, A. Vijayaraghavan, and K. Novoselov, "Graphene sensors," *IEEE Sensors J.*, vol. 11, no. 12, pp. 3161–3170, Dec. 2011.
- [20] J. Zhu, D. Yang, Z. Yin, Q. Yan, and H. Zhang, "Graphene and graphene-based materials for energy storage applications," *Small*, vol. 10, no. 17, pp. 3480–3498, Sep. 2014.
- [21] N. Petrone, I. Meric, T. Chari, K. L. Shepard, and J. Hone, "Graphene field-effect transistors for radio-frequency flexible electronics," *IEEE J. Electron Devices Soc.*, vol. 3, no. 1, pp. 44–48, Jan. 2015.
- [22] J. Perruisseau-Carrier, M. Tamagnone, J. S. Gomez-Diaz, and E. Carrasco, "Graphene antennas: Can integration and reconfigurability compensate for the loss?" in *Proc. EuMC*, Oct. 2013, pp. 369–372.
- [23] B. Wu and Y. Hao, "Material region division and antenna application of monolayer and multilayer graphene," in *Proc. EuCAP*, Apr. 2014, pp. 497–498.
- [24] D. Mishra and S. De, "Effects of practical rechargeability constraints on perpetual RF harvesting sensor network operation," *IEEE Access*, vol. 4, pp. 750–765, 2016.
- [25] Y. He, X. Cheng, W. Peng, and G. L. Stuber, "A survey of energy harvesting communications: Models and offline optimal policies," *IEEE Commun. Mag.*, vol. 53, no. 6, pp. 79–85, Jun. 2015.
- [26] M. Pinuela, P. D. Mitcheson, and S. Lucyszyn, "Ambient RF energy harvesting in urban and semi-urban environments," *IEEE Trans. Microw. Theory Techn.*, vol. 61, no. 7, pp. 2715–2726, Jul. 2013.
- [27] W. C. Brown, "The history of power transmission by radio waves," *IEEE Trans. Microw. Theory Techn.*, vol. 32, no. 9, pp. 1230–1242, Sep. 1984.
- [28] Y. Pan, C. V. Powell, A. M. Song, and C. Balocco, "Micro rectennas: Brownian ratchets for thermal-energy harvesting," *Appl. Phys. Lett.*, vol. 105, no. 25, pp. 253901–1–253901–4, Dec. 2014.
- [29] S.-E. Zhu, S. Yuan, and G. C. A. M. Janssen, "Optical transmittance of multilayer graphene," *Europhys. Lett.*, vol. 108, no. 1, pp. 17007-p1–17007-p4, 2014.
- [30] S. Bae *et al.*, "Roll-to-roll production of 30-inch graphene films for transparent electrodes," *Nature Nanotechnol.*, vol. 5, pp. 574–578, Jun. 2010.
- [31] W. Liu, J. Kang, and K. Banerjee, "Characterization of FeCl₃ intercalation doped CVD few-layer graphene," *IEEE Electron Device Lett.*, vol. 37, no. 9, pp. 1246–1249, Sep. 2016.
- [32] I. Khrapach *et al.*, "Novel highly conductive and transparent graphene-based conductors," *Adv. Mater.*, vol. 24, no. 21, pp. 2844–2849, 2012.
- [33] J. Li, F. Ye, S. Vaziri, M. Muhammed, M. C. Lemme, and M. Östling, "Efficient inkjet printing of graphene," *Adv. Mater.*, vol. 25, no. 29, pp. 3985–3992, Aug. 2013.
- [34] K. Leosson, A. S. Ingason, B. Agnarsson, A. Kossoy, S. Olafsson, and M. C. Gather, "Ultra-thin gold films on transparent polymers," *Nanophotonics*, vol. 2, no. 1, pp. 3–11, 2013.
- [35] C. A. Balanis, *Antenna Theory: Analysis and Design*. New York, NY, USA: Wiley, 1982.
- [36] C. A. Balanis, "Antenna theory: A review," *Proc. IEEE*, vol. 80, no. 1, pp. 7–23, Jan. 1992.

- [37] M. A. Andersson, A. Vorobiev, J. Sun, A. Yurgens, S. Gevorgian, and J. Stake, "Microwave characterization of Ti/Au-graphene contacts," *Appl. Phys. Lett.*, vol. 103, no. 17, pp. 173111-1–173111-4, 2013.
- [38] H. S. Skulason et al., "110 GHz measurement of large-area graphene integrated in low-loss microwave structures," *Appl. Phys. Lett.*, vol. 99, no. 15, pp. 153504-1–153504-3, 2011.
- [39] S. A. Awan et al., "Transport conductivity of graphene at RF and microwave frequencies," *2D Mater.*, vol. 3, no. 1, pp. 015010-1–015010-11, Feb. 2016.
- [40] Z. Popović et al., "Scalable RF energy harvesting," *IEEE Trans. Microw. Theory Techn.*, vol. 62, no. 4, pp. 1046–1056, Apr. 2014.
- [41] S. Hemour and K. Wu, "Radio-frequency rectifier for electromagnetic energy harvesting: Development path and future outlook," *Proc. IEEE*, vol. 102, no. 11, pp. 1667–1691, Nov. 2014.
- [42] M. A. Andersson and J. Stake, "An accurate empirical model based on Volterra series for FET power detectors," *IEEE Trans. Microw. Theory Techn.*, vol. 64, no. 5, pp. 1431–1441, May 2016.
- [43] A. Zak et al., "Antenna-integrated 0.6 THz FET direct detectors based on CVD graphene," *Nano Lett.*, vol. 14, no. 10, pp. 5834–5838, 2014.
- [44] Z. Zhang, R. Rajavel, P. Deelman, and P. Fay, "Sub-micron area heterojunction backward diode millimeter-wave detectors with $0.18\text{pW/Hz}^{1/2}$ noise equivalent power," *IEEE Microw. Compon. Lett.*, vol. 21, no. 5, pp. 267–269, May 2011.
- [45] C. H. P. Lorenz et al., "Breaking the efficiency barrier for ambient microwave power harvesting with heterojunction backward tunnel diodes," *IEEE Trans. Microw. Theory Techn.*, vol. 63, no. 12, pp. 4544–4555, Dec. 2015.
- [46] C. Song, Y. Huang, J. Zhou, J. Zhang, S. Yuan, and P. Carter, "A high-efficiency broadband rectenna for ambient wireless energy harvesting," *IEEE Trans. Antennas Propag.*, vol. 63, no. 8, pp. 3486–3495, Aug. 2015.
- [47] T. Tirronen, A. Larmo, J. Sachs, B. Lindoff, and N. Wiberg, "Machine-to-machine communication with long-term evolution with reduced device energy consumption," *Trans. Emerg. Telecommun. Technol.*, vol. 24, no. 4, pp. 413–426, 2013.
- [48] P. P. Mercier, S. Bandyopadhyay, A. C. Lysaght, K. M. Stankovic, and A. P. Chandrakasan, "A sub-nW 2.4 GHz transmitter for low data-rate sensing applications," *IEEE J. Solid-State Circuits*, vol. 49, no. 7, pp. 1463–1474, Jul. 2014.
- [49] T. Paing, E. A. Falkenstein, R. Zane, and Z. Popović, "Custom IC for ultralow power RF energy scavenging," *IEEE Trans. Power Electron.*, vol. 26, no. 6, pp. 1620–1626, Jun. 2011.
- [50] A. Dolgov, R. Zane, and Z. Popović, "Power management system for online low power RF energy harvesting optimization," *IEEE Trans. Circuits Syst. I, Reg. Papers*, vol. 57, no. 7, pp. 1802–1811, Jul. 2010.



the development of fabrication and modeling techniques for graphene-based transistors and circuits at microwave and terahertz frequencies.



Technology, Gothenburg, Sweden. Her research interests are in the areas of energy harvesting, statistical signal processing, communications, and optimization.

MICHAEL A. ANDERSSON (S'12) was born in Varberg, Sweden, in 1988. He received the B.Sc. degree in electrical engineering and the M.Sc. degree in wireless and photonics engineering from the Chalmers University of Technology in 2010 and 2012, respectively. He is currently pursuing the Ph.D. degree with the Terahertz and Millimetre Wave Laboratory, Department of Microtechnology and Nanoscience, Chalmers University of Technology. His research focuses on

AYÇA ÖZÇELIKKALE (M'10) received the B.Sc. degree in electrical engineering and a double major B.A. degree in philosophy from the Middle East Technical University, Ankara, Turkey, and the M.S. and Ph.D. degrees in electrical engineering from Bilkent University, Ankara. She spent part of her doctoral studies with the Department of Mathematics and Statistics, Queens University, Kingston, ON, Canada. She is currently a Post-Doctoral Researcher with Chalmers University of



istic channel modeling.

MARTIN JOHANSSON (M'93–SM'06) received the M.S. degree in engineering physics and the Ph.D. degree in electromagnetics from the Chalmers University of Technology in 1986 and 1997, respectively. He joined Ericsson Research, Ericsson AB, Gothenburg, Sweden, in 1997, where he currently serves as an Expert in antenna technology. His current research interests include antenna technology for mobile communications, antenna system modeling, and determin-



ULRIKA ENGSTRÖM received the M.S. degree in physics and engineering physics and the Ph.D. degree in physics from the Chalmers University of Technology in 1994 and 1999, respectively. She joined Ericsson Research, Ericsson AB, Gothenburg, Sweden, in 1999, where she is currently a Team Leader as part of Ericsson's 5G Research. Her current research interests include 5G systems with a focus on antenna systems for mobile communications and new use cases for 5G.



the Chalmers University of Technology. His main research interests are in development and application of emerging functional materials and phenomena in microwave devices. His current activities focus on materials, technology, and design of graphene-based field-effect transistors and components/systems for microwave/terahertz applications.

ANDREI VOROBIEV received the M.Sc. degree in physics of semiconductors and dielectrics from Gorky State University, Gorky, Russia, in 1986, and the Ph.D. degree in physics and mathematics from the Institute for Physics of Microstructures, Russian Academy of Sciences, Nizhny Novgorod, Russia, in 2000. In 2008, he was an Associate Professor in physical electronics from the Chalmers University of Technology, Gothenburg, Sweden. He currently holds a Senior Research Chair with



Laboratory, Didcot, U.K. He then joined Saab Combitech Systems AB as a Senior RF/microwave Engineer, until 2003. From 2000 to 2006, he held different academic positions with the Chalmers University of Technology, and from 2003 to 2006, he was also the Head of the Nanofabrication Laboratory, Department of Microtechnology and Nanoscience. In 2007, he was a Visiting Professor with the Submillimeter Wave Advanced Technology Group, Caltech/JPL, Pasadena, USA. He is currently a Professor and the Head of the Terahertz and Millimetre Wave Laboratory, Chalmers University of Technology, Sweden. He is also the Co-Founder of Wasa Millimeter Wave AB, Göteborg. His research involves graphene electronics, high-frequency semiconductor devices, terahertz electronics, submillimeter wave measurement techniques (terahertz metrology), and terahertz in biology and medicine. He serves as the Editor-in-Chief of the IEEE Transactions on Terahertz Science and Technology.

JAN STAKE (S'95–M'00–SM'06) was born in Uddevalla, Sweden, in 1971. He received the M.Sc. degree in electrical engineering and the Ph.D. degree in microwave electronics from the Chalmers University of Technology, Göteborg, Sweden, in 1994 and 1999, respectively. In 1997, he was a Research Assistant with the University of Virginia, Charlottesville, USA. From 1999 to 2001, he was a Research Fellow with the Millimetre Wave Group, Rutherford Appleton